Zeeman splittings near the *L* point of the Brillouin zone in zinc-blende semiconductors

K. Ando, H. Saito, M. C. Debnath, and V. Zayets
Nanoelectronics Research Institute, AIST, Tsukuba Central 2, Umezono 1-1-1, Tsukuba, Ibaraki 305-8568, Japan

A. K. Bhattacharjee
Laboratoire de Physique des Solides, UMR du CNRS, Université Paris-Sud, 91405 Orsay, France
(Received 26 November 2007; published 17 March 2008)

We report the effective interband g factors of the E_1 and $E_1+\Delta_1$ transitions in GaAs, CdTe, ZnTe, and ZnSe. They have been deduced from a combined measurement of the optical absorption and the magnetic circular dichroism spectra. A calculation of the g factors based on a 12-band $\mathbf{k}\cdot\mathbf{p}$ theory is also presented. It provides a satisfactory interpretation of the experimental values.

DOI: 10.1103/PhysRevB.77.125123 PACS number(s): 78.20.Ls, 78.40.Fy, 71.70.Ej, 71.20.Nr

I. INTRODUCTION

Magneto-optical spectra of semiconductors contain much information for understanding the electronic structure. Diluted magnetic semiconductors (DMSs) based on II-VI and III-V compounds are among the best examples which demonstrate the usefulness of the magneto-optical spectroscopy.[1,2] Magneto-optical signals not only from near the Γ critical point of the Brillouin zone but also from the *L* critical point play an important role in elucidating the physics of DMSs.[3] However, the Zeeman splittings at the *L* point of the nonmagnetic host semiconductors have not yet been well characterized. A knowledge of the associated g factors at the secondary extrema of the bands seems also of interest for possible spin manipulations in nanostructures.

Indeed, studies of the magneto-optical properties at the *L* point have been very limited. Fujimori *et al.*[4] reported the modulated reflectance and the magnetic circular dichroism (MCD) spectra around the E_1 and $E_1+\Delta_1$ transitions in InSb, Ge, and GaAs. By analyzing the MCD spectra, they obtained the effective interband g factors (g_{eff}) of both transitions. In InSb and Ge, both $g_{\text{eff}}(E_1)$ and $g_{\text{eff}}(E_1+\Delta_1)$ are negative. However, in GaAs, they show different polarities: $g_{\text{eff}}(E_1)<0$ and $g_{\text{eff}}(E_1+\Delta_1)>0$. As Fujimori *et al.*[4] pointed out, a theoretical calculation[5] of the effective g factors by using the simple six-band $\mathbf{k}\cdot\mathbf{p}$ theory at the *L* point of the Brillouin zone always predicts negative values. In order to explain the discrepancy between the experimental result and the theoretical expectation in GaAs, they assumed that the critical point for the transitions was located at a Λ point closer to the zone center (Γ) than to the zone boundary (*L*). However, this is clearly in contradiction with the present-day knowledge of the band structure, which locates this critical point at or near the *L* point in GaAs and the other compound semiconductors.[6,7] Thus, the observed "anomaly" in GaAs basically remains unexplained.

In this work, we report an experimental and theoretical study of the MCD spectra in GaAs and a series of II-VI semiconductors, typically used as host materials for the synthesis of DMSs, in order to determine the effective g factors at (or near) the *L* point and contribute to their interpretation.

II. EXPERIMENT

Thin films of ZnTe, ZeSe, CdTe, and GaAs were grown on sapphire ⟨0001⟩ substrate by using the molecular beam epitaxy method. The growth temperatures of ZnTe, ZeSe, CdTe, and GaAs are 350, 250, 240, and 600 °C, respectively. The films grew in the ⟨111⟩ direction. Their thickness ranged from 40 to 70 nm. The optical absorption spectra were measured by using the two-beam method at 6 K. The MCD spectra were also measured at 6 K in the transmission configuration by modulating the circular polarization between σ_+ and σ_- (see Fig. 1). A magnetic field of 10 kG was applied along the light propagation direction for the MCD measurements.

The MCD angle Θ and the optical absorption coefficient k are related by the equation[1]

$$\Theta = -\frac{45}{\pi}\Delta(E)\frac{dk}{dE}L, \tag{1}$$

where $\Delta(E)\equiv E(\sigma_-)-E(\sigma_+)$ is the Zeeman splitting at the photon energy E and L the sample thickness. Following Ref. 4, we define g_{eff}, the effective interband g factor, by

$$\Delta(E) \equiv -g_{\text{eff}}\mu_B H, \tag{2}$$

where μ_B is the Bohr magneton and H the applied field.

The values of g_{eff} can be deduced by comparing the MCD and the energy derivative of absorption: $\frac{d(kL)}{dE}$. Because the MCD signal intensity is proportional to L, the obtained values of g_{eff} are independent of the sample thickness.

The optical absorption spectra of GaAs, CdTe, ZnTe, and ZnSe at 6 K are presented in Fig. 2. Each spectrum shows two peaks identified as the E_1 and $E_1+\Delta_1$ transitions. They

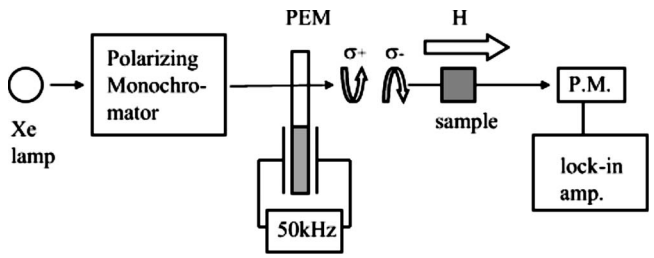

FIG. 1. Experimental setup to measure magnetic circular dichroism (MCD): Alternating σ_+ and σ_- circularly polarized light is generated by a photoelastic modulator. Polarization dependent optical absorption of a sample in a magnetic field H is detected by a photomultiplier and a lock-in amplifier.

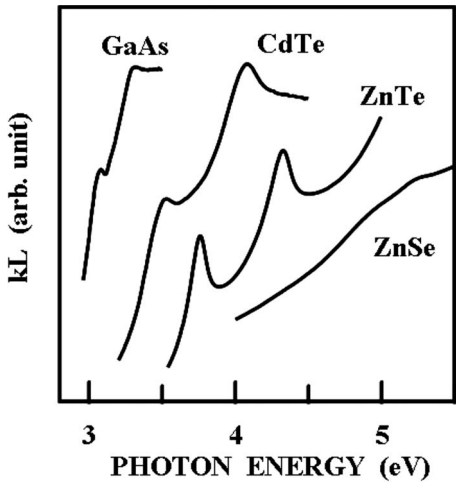

FIG. 2. The optical absorption spectra of GaAs, CdTe, ZnTe, and ZnSe at 6 K.

are quite sharp except in ZnSe. The spectra of the energy derivative of absorption presented below were computed from these curves.

The MCD and the energy derivative of absorption in ZnTe are presented in Fig. 3. Previously reported transition energies[7] measured at 300 K are shown by the vertical lines. Both spectra clearly show a dispersive shape as expected from Eq. (1). These dispersive spectral shapes of the MCD and the optical absorption derivative have the same polarity at both E_1 and $E_1+\Delta_1$. Thus, we have a positive g_{eff} for both transitions in ZnTe. A quantitative comparison between the two curves leads to the corresponding values of g_{eff}, as shown in Table I.

Figures 4 and 5 show the MCD and the energy derivative of absorption in ZnSe and CdTe, respectively. The vertical bars again indicate the energies of E_1 and $E_1+\Delta_1$ previously measured at 300 and 77 K, respectively.[7] As in ZnTe, the g_{eff} values are again both positive in the two systems (see Table I).

Figure 6 shows the MCD and the energy derivative of absorption in GaAs. The transition energies shown by the vertical bars were measured at 22 K.[7] In this compound, the g factor changes sign: $g_{\text{eff}}(E_1)$ is negative but $g_{\text{eff}}(E_1+\Delta_1)$ is positive, in accord with Ref. 4.

TABLE I. Effective interband g factors of E_1 and $E_1+\Delta_1$ transitions.

Compound	$g_{\text{eff}}(E_1)$	$g_{\text{eff}}(E_1+\Delta_1)$
ZnTe	$+0.3\pm0.05$	$+1.2\pm0.1$
ZnSe	$+0.7\pm0.1$	$+0.6\pm0.2$
CdTe	$+0.9\pm0.05$	$+1.2\pm0.1$
GaAs	-1.0 ± 0.1	$+2.0\pm0.2$

III. THEORY

The point group of a zinc-blende-structure crystal is T_d. At a Λ or L point of the Brillouin zone, the symmetry group of the wave vector $\mathbf{k}$ is C_{3v}. The first conduction band in a III-V or II-VI semiconductor is a Λ_1 singlet and the upper valence band a Λ_3 doublet, in the usual notations. When spin is considered, the former becomes the doubly degenerate Λ_6 and the latter is split by the spin-orbit interaction into two doublets: $\Lambda_{4,5}$ lying above Λ_6. In fact, the irreducible representations Λ_4 and Λ_5, which are related by the time-reversal symmetry, are exactly degenerate only at the zone center and the zone boundary $\Lambda=L$.[5] We study the Zeeman splitting of the optical transitions $\Lambda_{4,5}^v\rightarrow\Lambda_6^c$ and $\Lambda_6^v\rightarrow\Lambda_6^c$, which correspond to the E_1 and $E_1+\Delta_1$ structures, respectively. In a magnetic field $\mathbf{H}$, the effective Zeeman Hamiltonian for each of the doublets involved can be written as

$$\mathcal{H}_Z^i=\mu_B g_i^{\parallel}H_z s_z+\mu_B g_i^{\perp}(H_x s_x+H_y s_y), \tag{3}$$

where s is the electron spin and g_i the band g factors with $i=c,45,6$ in obvious notations. Note that in all the compounds under consideration, the Zeeman splittings are much smaller than the spin-orbit splitting Δ_1 and the valence band doublets can also be treated independently of each other. We have chosen the z axis along the $\langle 111\rangle$ direction, the axis of C_{3v} symmetry.

We calculate the Zeeman splittings in a sraightforward manner following the symmetry-based method of Ref. 3. According to the known band structure, the critical point $\Lambda\simeq L$, so the zero-field splitting of $\Lambda_{4,5}$ is neglected. Each $\mathcal{H}_Z^i$ matrix is written down in the corresponding basis

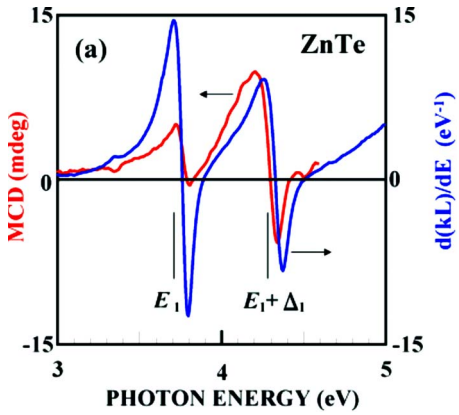

FIG. 3. (Color online) MCD and the energy derivative of absorption in ZnTe at $T=6$ K and $H=1$ T.

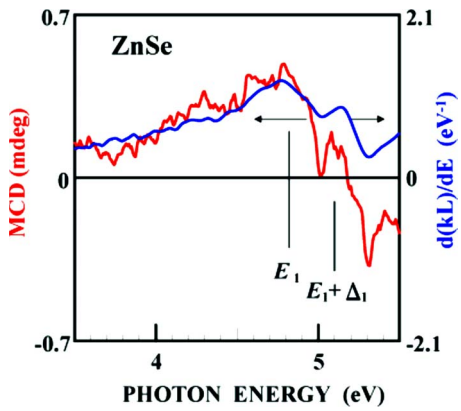

FIG. 4. (Color online) MCD and the energy derivative of absorption in ZnSe at $T=6$ K and $H=1$ T.

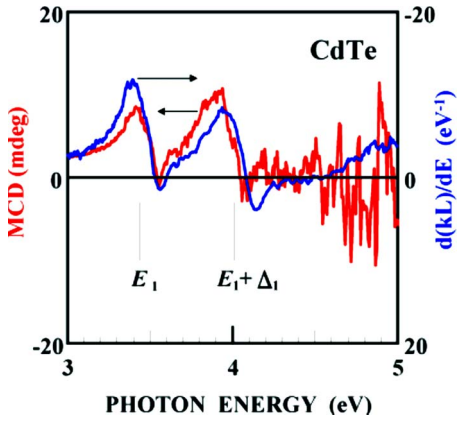

FIG. 5. (Color online) MCD and the energy derivative of absorption in CdTe at $T=6$ K and $H=1$ T.

(see Ref. 3) and diagonalized. For a general orientation (θ,ϕ) of the applied field, each of the transitions E_1 and $E_1+\Delta_1$ splits into four components which are allowed in both σ_+ and σ_- polarizations. As such a fine structure cannot be experimentally resolved, we calculate the weighted average $\langle E\rangle$ of the energy of the four components in a given polarization, the weights being the relative oscillator strengths. The average Zeeman splitting of the transition is then $\langle\Delta E\rangle=\langle E(\sigma_-)\rangle-\langle E(\sigma_+)\rangle$. We obtain

$$\frac{\langle\Delta(E_1)\rangle}{\mu_B H}=\frac{2\cos^2\theta}{1+\cos^2\theta}(g_c^{\parallel}-g_{45}^{\parallel}), \tag{4}$$

$$\frac{\langle\Delta(E_1+\Delta_1)\rangle}{\mu_B H}=-\frac{2\cos^2\theta}{1+\cos^2\theta}(g_c^{\parallel}-g_6^{\parallel}). \tag{5}$$

Note that the transverse g factors do not appear in Eqs. (4) and (5). Those of the valence bands simply drop out in the corresponding $\mathcal{H}_Z$ matrices. Also, $g_c^{\perp}$ disappears in the process of averaging over the components described above; this is related to the selection rules. Here, θ is the angle between the field and the $\langle 111\rangle$ directions. Next, we average over the four L directions. Defining $r\equiv\langle 2\cos^2\theta/(1+\cos^2\theta)\rangle$ for this averaging, we finally obtain the Zeeman splittings: $\Delta(E_1)$

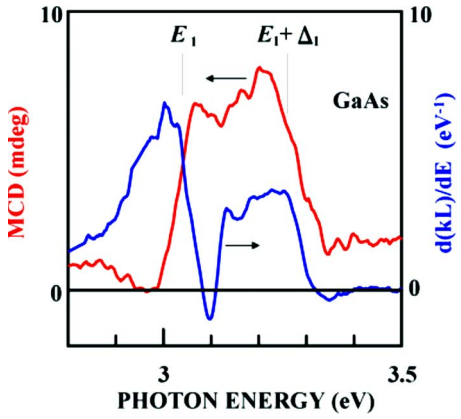

FIG. 6. (Color online) MCD and the energy derivative of absorption in GaAs at $T=6$ K and $H=1$ T.

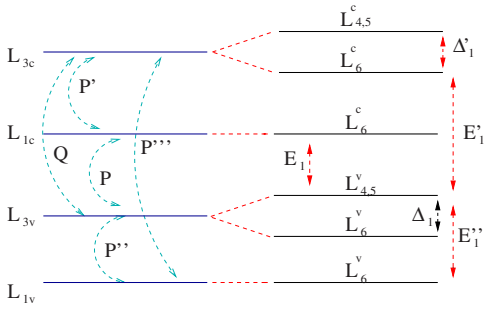

FIG. 7. (Color online) Schematic diagram of the band structure at the L point. The broken arcs in the left panel indicate the momentum matrix elements. The left (right) panel shows the single-group (double-group) irreducible representations. The E and Δ denote the energy gaps and the spin-orbit splittings, respectively.

$=r(g_c^{\parallel}-g_{45}^{\parallel})\mu_B H$ and $\Delta(E_1+\Delta_1)=-r(g_c^{\parallel}-g_6^{\parallel})\mu_B H$, where $r=1/2$ for H along $\langle 100\rangle$, $r=2/5$ for H along $\langle 111\rangle$ or $\langle 110\rangle$, and $r=(4-\pi)/2$ for a random orientation of the field.[3] Thus, the effective interband g factors as defined in Eq. (2) are given by

$$g_{\mathrm{eff}}(E_1)=-r(g_c^{\parallel}-g_{45}^{\parallel}),\quad g_{\mathrm{eff}}(E_1+\Delta_1)=+r(g_c^{\parallel}-g_6^{\parallel}). \tag{6}$$

We finally calculate the band g factors $g_i^{\parallel}$ in the $\mathbf{k}\cdot\mathbf{p}$ approximation following Roth's formula.[8] Figure 7 presents a schematic diagram of the band structure at the L point explicitly showing the 12 bands (states) taken into account. It follows the known band structure of these compounds.[6] In addition to the conduction band L_{1c} and the valence band L_{3v}, we include the upper conduction band L_{3c} and the lower valence band L_{1v}. Note the differences with respect to the band structure assumed in Ref. 4. Moreover, we update the theory and include the off-diagonal spin-orbit coupling Δ^- (see Ref. 9 and references therein). Thus,

$$\begin{aligned} g_c^{\parallel}=2&-\left(\frac{2P^2}{m}\right)\frac{\Delta_1}{E_1(E_1+\Delta_1)}\\ &-\left(\frac{2P'^2}{m}\right)\frac{\Delta_1'}{(E_1'-E_1)(E_1'+\Delta_1'-E_1)}\\ &+\left(\frac{4PP'}{3m}\right)\Delta^-\left[\frac{1}{E_1(E_1'+\Delta_1'-E_1)}+\frac{1}{(E_1+\Delta_1)(E_1'-E_1)}\right], \end{aligned} \tag{7}$$

$$\begin{aligned} g_{45}^{\parallel}=2&-\frac{2}{mE_1}\left[P^2-\left(\frac{2PP'}{3}\right)\frac{\Delta^-}{E_1'+\Delta_1'}\right]\\ &+\frac{2}{mE_1''}\left[P''^2-\left(\frac{2P''P'''}{3}\right)\frac{\Delta^-}{E_1'+\Delta_1'}\right]+\frac{4Q^2}{mE_1'}, \end{aligned} \tag{8}$$

$$g_6^{\parallel} = 2 + \frac{2}{m(E_1+\Delta_1)}\left[P^2 + \left(\frac{2PP'}{3}\right)\frac{\Delta^-}{E_1'+\Delta_1}\right] - \frac{2}{m(E_1''-\Delta_1)}\left[P''^2 + \left(\frac{2P''P'''}{3}\right)\frac{\Delta^-}{E_1'+\Delta_1}\right] - \frac{4Q^2}{m(E_1'+\Delta_1'+\Delta_1)}. \quad (9)$$

Note that the sign of g_6 as defined by us is opposite to that used in Ref. 4. Moreover, we have dropped the intraband momentum matrix element $\Pi \equiv -\langle X(L_{3v}|p_y|X(L_{3v})\rangle$, crucial to the discussion of Fujimori *et al.* because it vanishes at L by symmetry and is negligibly small at $\Lambda \simeq L$. The symbols used above for the energy gaps, spin-orbit splittings, and momentum matrix elements, indicated in Fig. 7, are analogous to the standard ones in the Γ-point 14-band $\mathbf{k}\cdot\mathbf{p}$ theory.[9] Explicitly, $P=i\langle X(L_{3v})|p_x|S(L_{1c})\rangle$, $P'=i\langle X(L_{3c})|p_x|S(L_{1c})\rangle$, $Q=i\langle Y(L_{3v})|p_x|X(L_{3c})\rangle$, and $\Delta^-=-3i\langle X(L_{3v})|l_y|Z(L_{3c})\rangle$, where $\mathbf{l}\equiv(\hbar/4m^2c^2)(\nabla V\times\mathbf{p})$. Unlike Fujimori *et al.*, who calculated the momentum matrix elements at the critical point starting from a Γ-point $\mathbf{k}\cdot\mathbf{p}$ approximation, we treat them as semiempirical parameters. As shown recently, the 14-band $\mathbf{k}\cdot\mathbf{p}$ theory at Γ is utterly inadequate for providing a correct description of the band structure far from the zone center.[10]

Obtaining a quantitative estimate of the g factors at the L point is, however, considerably more difficult than at Γ. In the latter case, experimental values of the energy denominators and those of the effective masses allow one to estimate the momentum matrix elements. In contrast, the experimental input at L in the present systems is basically limited to the energies E_1 and $E_1+\Delta_1$. We shall additionally use the calculated energy values from the semiconductor data handbook.[7] In cases where Δ_1' is not available, we approximate it by $\frac{2}{3}\Delta_0'$, following the two-thirds rule. The L-point effective mass measurements in some systems indicate that the matrix elements P and P' are roughly equal to those at the Γ point.[11] In fact, the dominant contributions to these matrix elements as well as to Q and Δ^- come from the atomic core region, making them slowly varying functions of $\mathbf{k}$. We, therefore, use the Γ-point values[9,12] of these four parameters. However, the additional momentum matrix elements $P'' \equiv i\langle X(L_{3v})|p_x|S(L_{1v})\rangle$ and $P''' \equiv i\langle X(L_{3c})|p_x|S(L_{1v})\rangle$ appearing here are more difficult to estimate. The L_{1v} state certainly contains contributions from lower bands at Γ. It turns out that only P'' appears in a numerically significant term in the calculated g factors. We leave it as an adjustible parameter, keeping in mind that it is expected to be much smaller than P. As $\mathbf{H}\|\langle 111\rangle$ in our experiments, we have $r=2/5$. In Table II, we present the calculated values of the effective interband g factors.

TABLE II. Estimated values of the effective g factors of the E_1 and $E_1+\Delta_1$ transitions, with the parameter $E_{P''}\equiv 2P''^2/m$ expressed in eV.

Compound	$g_{\mathrm{eff}}(E_1)$	$g_{\mathrm{eff}}(E_1+\Delta_1)$
ZnTe	$0.019+0.090E_{P''}$	$-0.461+0.103E_{P''}$
ZnSe	$-0.154+0.090E_{P''}$	$-0.325+0.095E_{P''}$
CdTe	$-0.465+0.098E_{P''}$	$-1.127+0.114E_{P''}$
GaAs	$-1.708+0.071E_{P''}$	$-2.091+0.074E_{P''}$

A comparison between Tables I and II shows that the calculated value of $g_{\mathrm{eff}}(E_1+\Delta_1)$ is systematically smaller than that of $g_{\mathrm{eff}}(E_1)$ in all the compounds. Experimentally, this is true only in ZnSe, but the difference between the two g factors is rather small in ZnSe and CdTe. Nevertheless, the positive sign of both g factors in the II-VI compounds is compatible with a value of $E_{P''}\equiv(2P''^2/m)<10$ eV, which is very reasonable. On the other hand, in the III-V compound GaAs, we can fit the negative experimental value of $g_{\mathrm{eff}}(E_1)$ with $E_{P''}\simeq 10$ eV. However, we cannot account for the positive sign of $g_{\mathrm{eff}}(E_1+\Delta_1)$ with a consistent value of $E_{P''}$. Thus, except for this case, we can explain the sign and order of magnitude of all the interband g factors measured by us. The discrepancies are perhaps related to the assumption of $\mathbf{k}$-independent values of the principal momentum matrix elements and/or the calculated energy denominators. An atomistic band structure calculation is in progress for a more quantitative theoretical estimate of the g factors. At this point, we can say that the 12-band $\mathbf{k}\cdot\mathbf{p}$ calculation presented here provides a reasonable framework for the interpretation of the observed Zeeman splittings.

IV. CONCLUDING REMARKS

We have measured the Zeeman splittings of the E_1 and $E_1+\Delta_1$ transitions in a series of compounds which are often used for synthesizing diluted magnetic semiconductors. Calculations based on a 12-band $\mathbf{k}\cdot\mathbf{p}$ model at the L point are shown to provide a rather satisfactory interpretation of the experimental data.

ACKNOWLEDGMENTS

A.K.B. wishes to thank the Nanoelectronics Research Institute for hospitality and the Japan Society for the Promotion of Science for financial support.

[1] K. Ando, in *Magneto-Optics*, edited by S. Sugano and N. Kojima, Springer Series in Solid-State Sciences Vol. 128 (Springer-Verlag, Berlin, 2000), p. 211.
[2] K. Ando, Science **312**, 1883 (2006).
[3] A. K. Bhattacharjee, Phys. Rev. B **41**, 5696 (1990).
[4] A. Fujimori, H. Fukutani, and G. Kuwabara, J. Phys. Soc. Jpn. **45**, 910 (1978).
[5] S. O. Sari, Phys. Rev. B **6**, 2304 (1972).
[6] M. L. Cohen and J. R. Chelikowsky, in *Electronic Structure and Optical Properties of Semiconductors*, edited by M. Cardona,

Springer Series in Solid-State Sciences Vol. 75 (Springer-Verlag, Berlin, 1989).

[7] *Semiconductors: Data Handbook*, edited by O. Madelung (Springer-Verlag, Berlin, 2003).

[8] L. M. Roth, B. Lax, and S. Zwerdling, Phys. Rev. **114**, 90 (1959); L. M. Roth, *ibid.* **118**, 1534 (1960).

[9] M. Cardona, N. E. Christensen, and G. Fasol, Phys. Rev. B **38**, 1806 (1988).

[10] J.-M. Jancu, R. Scholz, E. A. de Andrada e Silva, and G. C. La Rocca, Phys. Rev. B **72**, 193201 (2005).

[11] M. Cardona, J. Phys. Chem. Solids **24**, 1543 (1963).

[12] M. Willatzen, M. Cardona, and N. E. Christensen, Phys. Rev. B **51**, 17992 (1995).